Key Points:
- Undrogued drifters and plastic debris accumulate similarly in the subtropical gyres
- The accumulation is too fast to be due to Ekman convergence
- Inertial effects (i.e., of finite size and buoyancy) explain the accumulation

Supporting Information:
- Supporting Information S1

Correspondence to:
F. J. Beron-Vera,
fberon@rsmas.miami.edu

Inertia-induced accumulation of flotsam in the subtropical gyres

F. J. Beron-Vera[1], M. J. Olascoaga[2], and R. Lumpkin[3]

[1]Department of Atmospheric Sciences, Rosenstiel School of Marine and Atmospheric Science, University of Miami, Miami, Florida, USA, [2]Department of Ocean Sciences, Rosenstiel School of Marine and Atmospheric Science, University of Miami, Miami, Florida, USA, [3]Physical Oceanography Division, AOML/NOAA, Miami, Florida, USA

Abstract Recent surveys of marine plastic debris density have revealed high levels in the center of the subtropical gyres. Earlier studies have argued that the formation of great garbage patches is due to Ekman convergence in such regions. In this work we report a tendency so far overlooked of drogued and undrogued drifters to accumulate distinctly over the subtropical gyres, with undrogued drifters accumulating in the same areas where plastic debris accumulate. We show that the observed accumulation is too fast for Ekman convergence to explain it. We demonstrate that the accumulation is controlled by finite-size and buoyancy (i.e., inertial) effects on undrogued drifter motion subjected to ocean current and wind drags. We infer that the motion of flotsam in general is constrained by similar effects. This is done by using a newly proposed Maxey-Riley equation which models the submerged (surfaced) drifter portion as a sphere of the fractional volume that is submerged (surfaced).

1. Introduction

The purpose of this brief communication is twofold. First, we report, for the first time, that drogued and undrogued drifters tend to distribute differently in the subtropical gyres, with undrogued drifters accumulating in regions where microplastic density surveys indicate elevated levels of floating marine debris [*Cozar et al.*, 2014]. Second, we provide an explanation for this tendency using an appropriate reduced Maxey-Riley equation [*Maxey and Riley*, 1983; *Cartwright et al.*, 2010] for the motion of buoyant finite-size (i.e., inertial) spherical particles. Unlike the standard Maxey-Riley equation, used previously in oceanographic applications [*Tanga and Provenzale*, 1994; *Beron-Vera et al.*, 2015], the new equation derived here takes into account the combined effects of water and air drags. The water velocity is taken to be causally related to the air velocity, so the role of the Ekman transport in the accumulation of flotsam in the ocean gyres, proposed earlier [*Maximenko et al.*, 2012], can be unambiguously evaluated. This is attained by considering the water velocity as the surface ocean velocity output from an ocean general circulation model. The air velocity is in turn obtained from the wind velocity that forces the model. The present approach is dynamical, aimed at explaining observed behavior, and thus is fundamentally different than earlier probabilistic approaches [*Maximenko et al.*, 2012; *van Sebille et al.*, 2012], more concerned with reproducing observations.

2. Observed Accumulation

The drifter data were collected by the NOAA (National Oceanic and Atmospheric Administration) Global Drifter Program over the period 1979–2015 [*Lumpkin and Pazos*, 2007]. The drifter positions are satellite tracked by the *Argos* system or GPS (Global Positioning System). The drifters follow the SVP (Surface Velocity Program) design, consisting of a surface spherical float which is drogued at 15 m, to minimize wind slippage and wave-induced drift [*Sybrandy and Niiler*, 1991].

Figure 1 (top left) shows density difference (expressed as a signed number per degree squared) between drifters after a period of at least 1 year from deployment and at deployment for all drifters that remained drogued over the entire 1 year period. Figure 1 (top right) shows the same but after at least 1 year since the drifters lost their drogues. The initial positions are similarly homogeneously distributed. But there is a difference in the final positions: the undrogued drifters reveal a clearer tendency to accumulate in the subtropical gyres. The accumulation is most evident in the North and South Atlantic and Pacific gyres.
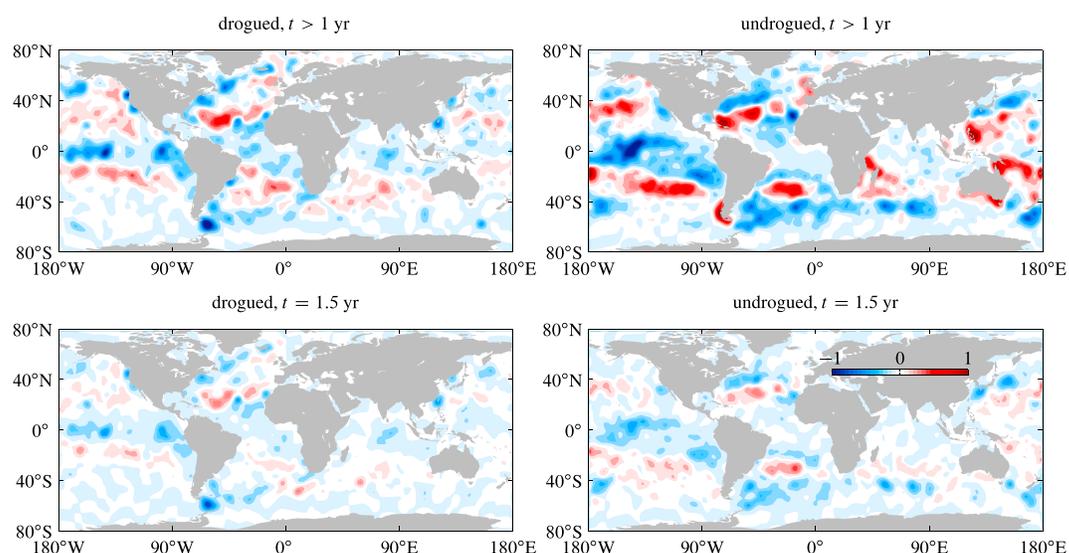
Figure 1. Expressed as a signed number per degree squared, density difference with respect to initial locations of (left column) drogued and (right column) undrogued drifters from the NOAA Global Drifter Program over 1979–2015 after at (top row) least 1 year or exactly (bottom row) 1.5 years past the time at deployment for drogued drifters or the location where a drifter loses the drogue.

The tendency of undrogued drifters to accumulate in the North and South Atlantic gyres is particularly robust as it is not influenced by the disparity in the amounts (1621 versus 2895) and mean lifetimes (1.5 versus 2 years) of the drogued and undrogued drifters used in the construction in Figure 1 (top row). This follows from the inspection in Figure 1 (bottom row), which shows the same as in Figure 1 (top row) but restricted to equal number of drifters (826, by random bootstrapping) and length of the trajectory records (1.5 year).

The reported accumulation tendency had been inferred earlier, but for both undrogued and drogued drifters and from the topology of ensemble-mean streamlines constructed using drifter velocities [*Maximenko et al.*, 2012]. These authors found their result unexpected given the different water-following characteristics of drogued and undrogued drifters [*Niiler and Paduan*, 1995]. The discrepancy with our finding may be attributed to errors in the drogue presence verification, which were discovered at the time of that publication and corrected in *Lumpkin et al.* [2012].

The accumulation inferred in *Maximenko et al.* [2012] was explained as a consequence of Ekman transport using steady flow arguments on fluid particle motion. In the next section we show that inertial effects provide an explanation for the accumulation when spherical float motion opposed by unsteady water and air flow drag is considered.

3. Simulated Accumulation

Consider a small spherical particle of radius a and density $\rho_p \leq \rho$, where ρ is the water density. The fraction of water volume displaced by the particle is δ^{-1}, where

$$\delta := \frac{\rho}{\rho_p}. \tag{1}$$

Posing the exact motion equation for a buoyant finite-size particle immersed in a fluid in motion is a challenging task [*Cartwright et al.*, 2010], which was solved to a very good approximation by *Maxey and Riley* [1983]. As a first step toward posing that for a particle at the air-sea interface, the more complicated case of interest here, we proceed heuristically by modeling the particle piece immersed in the water (air) as a sphere of the fractional volume that is immersed in the water (air) and assuming that it evolves according to the Maxey-Riley set. The subspheres are advected together and the forces acting on each of them are calculated at the

same position. Adding these forces as if they were decoupled from one another, we obtain (cf. supporting information, Text S1):

$$\ddot{x} + f\dot{x}^\perp = D_t v + f v^\perp - \frac{2\left(\gamma + \sqrt[3]{\delta - 1}\right)}{3\gamma\sqrt[3]{\delta}\tau}\left(\dot{x} - u\right),\tag{2}$$

where

$$u := \frac{\gamma v + \sqrt[3]{\delta - 1}\,v_a}{\gamma + \sqrt[3]{\delta - 1}}.\tag{3}$$

Here x denotes position on the horizontal plane, v and v_a are water and air velocities, $D_t := \partial_t + v \cdot \nabla$, f is the Coriolis parameter, and

$$\tau := \frac{2a^2}{9\nu\delta}, \quad \gamma := \frac{\nu\rho}{\nu_a\rho_a},\tag{4}$$

where ρ_a is the density of the air and ν and ν_a are water and air dynamic viscosities. The left-hand side of (2) is the absolute acceleration of the particle. The first and second terms on the right-hand side are flow and drag forces mediated by added mass effects, respectively, which water and air exert on the particle.

The Maxey-Riley equation (2) constitutes a nonautonomous four-dimensional dynamical system for the particle position and velocity, $v_p = \dot{x}$. To integrate it, one must specify both initial particle position and velocity, which is not known in general. In addition, long reversed-time integrations of (2), which are useful, for instance, in pollution source detection, are not feasible because the term $-\dot{x}/\tau$ produces exponential growth with exponent τ^{-1} for decreasing t. This tends to cause numerical instability as it has been noted earlier for the standard Maxey-Riley equation [*Haller and Sapsis*, 2008].

However, for a sufficiently small particle ($\tau \to 0$) the Maxey-Riley equation (2) reduces to (cf. supporting information, Text S1, Appendix B)

$$\dot{x} = v_p = u + \frac{3\gamma\sqrt[3]{\delta}\tau}{2\left(\gamma + \sqrt[3]{\delta - 1}\right)}\left(D_t v + f v^\perp - f u^\perp\right).\tag{5}$$

This equation, which will be referred to as an *inertial equation*, constitutes a two-dimensional system in the position and thus can be integrated without knowledge of the initial velocity. Also, it is not subjected to numerical instability in long backward-time integration. Up to an $O(\tau^2)$ error, the particle velocity is equal to a weighted average of the water and air velocities (u) plus a term proportional to the product of the particle timescale (τ) and the difference between the water absolute acceleration ($D_t v + f v^\perp$) and a Coriolis acceleration due to u.

To carry out the integration of (5) realizations of v and v_a near the ocean-atmosphere interface are needed. Here we have chosen to consider v as given by surface ocean velocity from the Global 1/12° HYCOM (HYbrid-Coordinate Ocean Model) + NCODA (Navy Coupled Ocean Data Assimilation) Ocean Reanalysis (GLBu0.08/expt_19.0) [*Cummings and Smedstad*, 2013]. In turn, we take v_a as the wind velocity from the National Centers for Environmental Prediction (NCEP) Climate Forecast System Reanalysis (CFSR), which is employed to construct the wind stress applied on the model. This way, ocean currents and winds employed in this study are dynamically consistent with each other.

Also needed for the integration of (5) are estimates of parameters γ, δ, and τ. For typical water and air density and viscosity values, $\gamma \approx 60$. From the configuration of the undrogued drifters we infer $\delta = 2$ (about half of the spherical float is submerged when the drogue is not present) and further estimate $\tau \approx 0.05$ day (the mean radius of the float is about 17.5 cm). Note that τ is small compared to relevant timescales such as the turnover time of a mesoscale eddy (a few days) or a subtropical gyre (a few years) [*Vallis*, 2006].

For the above velocity realizations and parameter choices we begin by integrating the inertial equation (5) using a Runge-Kutta method from a uniform distribution of particles. For comparison we also integrate $\dot{x} = v$ from the same positions. In both cases integrations are initialized along three simulation years (2005–2007). Starting on the drifter deployment positions or where the drifters lose their drogues on the corresponding
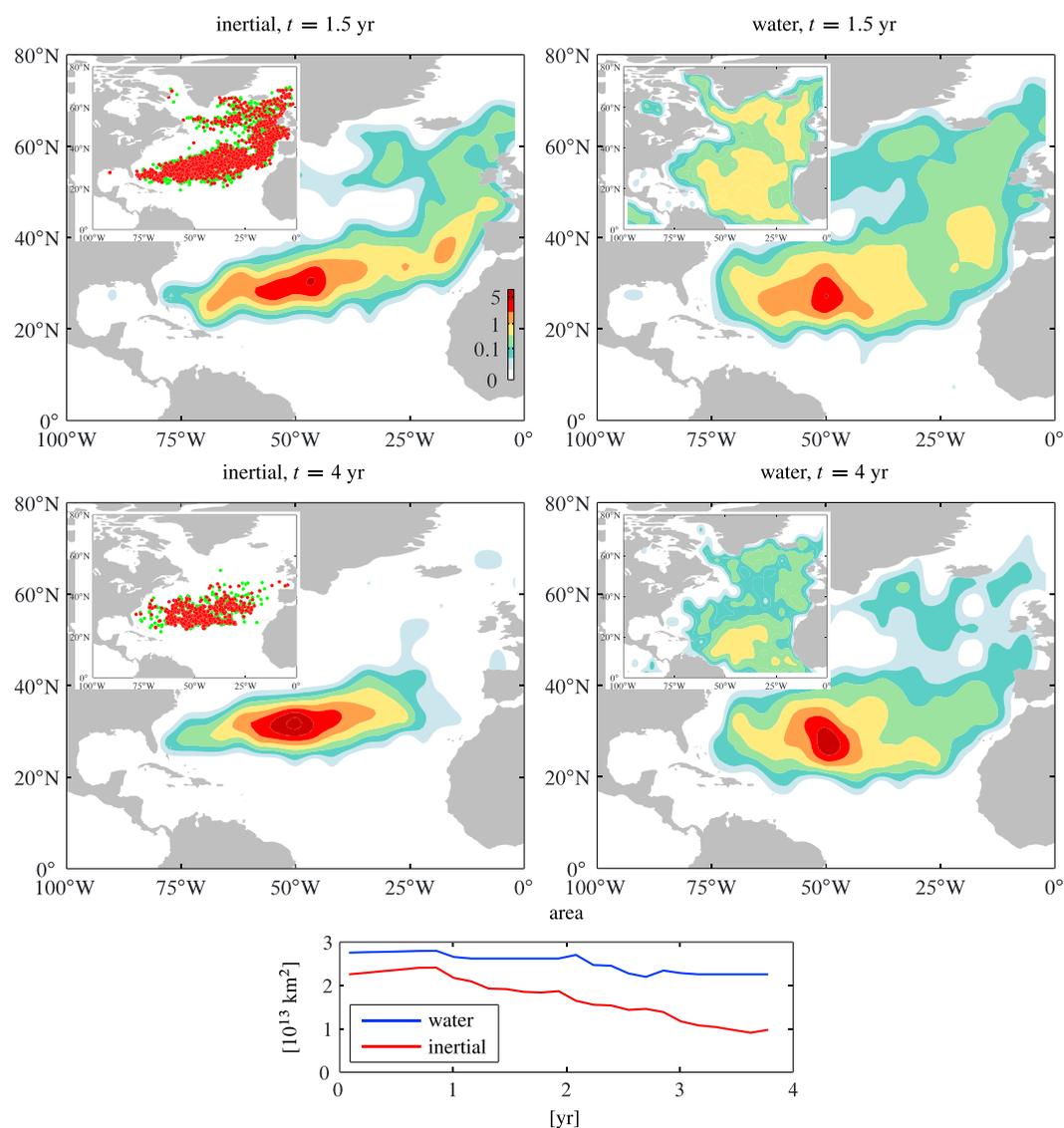
Figure 2. Density of particles after (top row) 1.5 and 4 (middle row) years of integration of the (left column) inertial equation (5) and of (right column) advection by water velocity normalized by density in the initially uniform distribution of particles. Insets in Figure 2 (left column) show final positions of inertial particles (red) and particles obeying the full Maxey-Riley equation (2) (green). Insets in Figure 2 (right column) show normalized density for particles advected by velocity derived geostrophically from sea surface height. (bottom) As function of time, area of the region where normalized particle density is higher than 1% for inertial (red) and water (blue) particles. Water velocity is given by surface ocean velocity from the 1/12° Global HYCOM+NCOM Ocean Reanalysis, from which sea surface height is also taken. The air velocity corresponds to the wind velocity from the NCEP/CFSR reanalysis used to construct the wind stress that forces the model.

dates is not possible because model output is not available over the entire drifter trajectory records. The proposed ensemble integrations facilitate intercomparisons and also guarantee robustness of the results. The integrations are carried over a period of 4 years, which is sufficiently long to reveal accumulation (undrogued drifters show clear signs of accumulation after about 1.5 year). For brevity we restrict the analysis to the North Atlantic; similar results are attained in the other basins (cf. supporting information, Figure S1).

The density (normalized by initial density) of inertial particles, i.e., controlled by (5), after 1.5 (Figure 2, top left) and 4 (Figure 2, middle left) years is high in the center of the subtropical gyre as is that of undrogued drifters. Note also (in the insets) that particles controlled by the Maxey-Riley equation (2) (green dots) take similar final distributions as inertial particles (red dots). This confirms the validity of (5), which attracts solutions of (2).
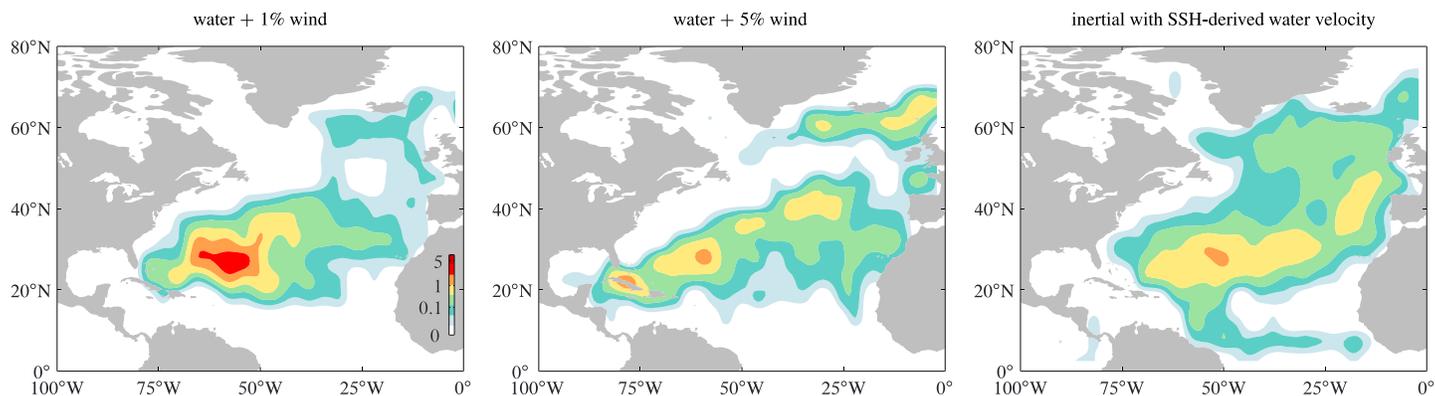
Figure 3. As in Figure 2 (top row) but for particles advected for 1.5 years using model velocity with (left) 1% and (middle) 5% windage added and (right) obeying the inertial equation (5) with the water velocity derived geostrophically from the model sea surface height output.

By contrast, after 1.5 year water particles, i.e., controlled by $\dot{x} = v$, take a more homogeneous distribution (Figure 2, top right), which is in better agreement with the distribution taken by drogued drifters . Accumulation in this case, most evident after 4 years (Figure 2, middle right), can be attributed to Ekman transport by comparing these distributions with the much more homogeneous distributions attained by the particles when v is taken as geostrophic (i.e., divergenceless) velocity inferred from the model sea surface height (SSH) field (insets).

Accumulation due to Ekman transport is a slow process. This is evident from the inspection in Figure 2 (bottom), which shows that the region where normalized particle density is higher than 1% decays nearly 2 times faster for inertial particles than for water particles. While there are not enough sufficiently long drogued drifter trajectories to verify this behavior, this is suggested by the application on such drifters of a probabilistic approach similar to that used earlier [*Maximenko et al.*, 2012; *van Sebille et al.*, 2012].

The behavior of the inertial particles just described can be anticipated by considering an idealized model of the large-scale circulation in the North Atlantic. In the simplest such models, due to *Stommel* [1966], the slow steady flow is divergenceless ($\nabla \cdot v = 0$) and has an anticyclonic basin-wide gyre, driven by strong steady westerlies and trade winds, so $\nabla \cdot v_a = 0$. Under such conditions,

$$\nabla \cdot v_p \approx \frac{3\gamma \sqrt[3]{\delta\tau}}{2\left(\gamma + \sqrt[3]{\delta-1}\right)^2} \sqrt[3]{\delta-1} f\omega_a, \tag{6}$$

where $\omega_a := -\nabla \cdot v_a^{\perp}$ is the air vorticity. Because $f\omega_a < 0$, (6) is negative, which promotes accumulation of inertial particles in the center of the gyre.

A pertinent question is if undrogued drifter accumulation may be inferred by simply considering $\dot{x} = v + \alpha v_a$ with $\alpha > 0$ small, an ad hoc model widely used to simulate windage effects on floating matter in the ocean [*Duhec et al.*, 2015]. Use of $\alpha = 0.01$ suggests that it may indeed be possible after 1.5 years of evolution (Figure 3, left), but use of a slightly larger value within the commonly used range such as $\alpha = 0.05$ reveals leakage of particles in the southwest direction (Figure 3, middle). This emphasizes the importance of finite-size effects. More specifically, for undrogued drifter parameters $u \approx 0.99 v + 0.02 v_a$ in (3), which incidentally is close to the ad hoc models just considered. This is the first term in the inertial equation (5). Finite-size effects are accounted for in the second term.

Another relevant question is if accumulation is revealed when SSH-derived instead of full v is used in the inertial equation (5). The relevance of this question stems from the wide use of satellite altimetry measurements of SSH in diagnosing surface ocean currents [*Fu et al.*, 2010]. The answer to the question is partially affirmative as the final particle position distribution reveals (Figure 3, right). A similar result is attained if altimetric SSH is employed.

4. Concluding Remarks

We conclude that undrogued drifters are quite strongly influenced by inertial effects. Drogued drifters, by contrast, appear to more closely follow the water motion. Ekman transport contributes to accumulate water,

but this acts on a longer time scale than inertial effects. We infer, then, that marine plastic debris, which accumulate in the same places as undrogued drifters, and flotsam in general must be affected by inertial effects in a similar manner as undrogued drifters.

We close by noting that shipwreck and airplane debris tracking, pollution source identification, and search and rescue operations at sea are among the many practical applications that may benefit from the use of the inertial equation derived here. Whether inaccuracies resulting from our heuristic derivation of this equation and omission of a number of potentially important processes (Stokes drift, infragravity waves, subgrid motions, etc.) or the quality of the velocity realizations will constrain more its success in such applications is a subject of ongoing research.

References

Beron-Vera, F. J., M. J. Olascoaga, G. Haller, M. Farazmand, J. Triñanes, and Y. Wang (2015), Dissipative inertial transport patterns near coherent Lagrangian eddies in the ocean, *Chaos*, *25*, 087412, doi:10.1063/1.4928693.

Cartwright, J. H. E., U. Feudel, G. Károlyi, A. de Moura, O. Piro, and T. Tél (2010), Dynamics of finite-size particles in chaotic fluid flows, in *Nonlinear Dynamics and Chaos: Advances and Perspectives*, edited by M. Thiel et al., pp. 51–87, Springer, Berlin.

Cozar, A., et al. (2014), Plastic debris in the open ocean, *Proc. Natl. Acad. Sci. U.S.A.*, *111*(28), 10,239–10,244, doi:10.1073/pnas.1314705111.

Cummings, J. A., and O. M. Smedstad (2013), Variational data analysis for the global ocean, in *Data Assimilation for Atmospheric, Oceanic and Hydrologic Applications*, vol. 2, edited by S. K. Park and L. Xu, chap. 13, pp. 303–343, Springer, Berlin, doi:10.1007/978-3-642-35088-7-13.

Duhec, A. V., R. F. Jeanne, N. Maximenko, and J. Hafner (2015), Composition and potential origin of marine debris stranded in the Western Indian Ocean on remote Alphonse Island, Seychelles, *Mar. Pollut. Bull.*, *96*(1–2), 76–86, doi:10.1016/j.marpolbul.2015.05.042.

Fu, L. L., D. B. Chelton, P.-Y. Le Traon, and R. Morrow (2010), Eddy dynamics from satellite altimetry, *Oceanography*, *23*, 14–25.

Haller, G., and F. J. Beron-Vera (2013), Coherent Lagrangian vortices: The black holes of turbulence, *J. Fluid Mech.*, *731*, R4, doi:10.1017/jfm.2013.391.

Haller, G., and F. J. Beron-Vera (2014), Addendum to 'Coherent Lagrangian vortices: The black holes of turbulence', *J. Fluid Mech.*, *755*, R3.

Haller, G., and T. Sapsis (2008), Where do inertial particles go in fluid flows?, *Physica D*, *237*, 573–583.

Lumpkin, R., and M. Pazos (2007), Measuring surface currents with Surface Velocity Program drifters: The instrument, its data and some recent results, in *Lagrangian Analysis and Prediction of Coastal and Ocean Dynamics*, edited by A. Griffa et al., chap. 2, pp. 39–67, Cambridge Univ. Press, Cambridge, U. K.

Lumpkin, R., S. A. Grodsky, L. Centurioni, M.-H. Rio, J. A. Carton, and D. Lee (2012), Removing spurious low-frequency variability in drifter velocities, *J. Atmos. Oceanic Technol.*, *30*, 353–360, doi:10.1175/JTECH-D-12-00139.1.

Maxey, M. R., and J. J. Riley (1983), Equation of motion for a small rigid sphere in a nonuniform flow, *Phys. Fluids*, *26*, 883–889.

Maximenko, A. N., J. Hafner, and P. Niiler (2012), Pathways of marine debris derived from trajectories of Lagrangian drifters, *Mar. Pollut. Bull.*, *65*, 51–62.

Niiler, P. P., and J. D. Paduan (1995), Wind-driven Motions in the northeastern Pacific as measured by Lagrangian drifters, *J. Phys. Oceanogr.*, *25*, 2819–2830.

Provenzale, A. (1999), Transport by coherent barotropic vortices, *Annu. Rev. Fluid Mech.*, *31*, 55–93.

Ripa, P. (1997), "Inertial" oscillations and the β-plane approximation(s), *J. Phys. Oceanogr.*, *27*, 633–647.

Stommel, H. (1966), *The Gulf Stream*, 2nd ed., Univ. of California, Los Angeles, Calif.

Sybrandy, A. L., and P. P. Niiler (1991), WOCE/TOGA Lagrangian drifter construction manual, Tech. Rep. SIO Reference 91/6, Scripps Inst. of Oceanogr., La Jolla, Calif.

Tanga, P., and A. Provenzale (1994), Dynamics of advected tracers with varying buoyancy, *Physica D*, *76*, 202–215.

Vallis, G. K. (2006), *Atmospheric and Oceanic Fluid Dynamics*, Cambridge Univ. Press, Cambridge, U. K.

van Sebille, E., E. H. England, and G. Froyland (2012), Origin, dynamics and evolution of ocean garbage patches from observed surface drifters, *Environ. Res. Lett.*, *7*, 044040.